

Antimatter Enigma Solved: Astronomical Data Allows Identification of 77 Supermassive Antimatter Black Holes and 23 Antimatter Galaxies.

Policarpo Yoshin Ulianov
poliyu77@gmail.com

Abstract

This article analyzes astronomical data that correlates the mass of 100 supermassive black holes (SMBHs) with the mass of the galaxies in which they are situated. A theoretical value is presented to calculate the logarithmic relationship $\log(\text{Galaxy Mass} / \text{SMBH Mass})$, which equals 2.963 for SMBHs composed of antimatter and 2.285 for galaxies of antimatter containing matter SMBHs. This theoretical relationship was calculated by the authors within the Ulianov Theory, considering the hypothesis of galaxy formation from matter (protons and electrons) expelled by antimatter SMBHs during cosmic inflation, as well as the hypothesis of galaxy formation from antimatter (antiprotons and positrons) expelled by matter SMBHs, also occurring during cosmic inflation. This value was experimentally observed based on the masses of 100 SMBHs and the masses of 100 galaxies in which they are situated. From this total, it was observed that 77% of the SMBHs are composed of antimatter, measuring a value of $(2.931 \pm 1.8\%)$ for the logarithmic relationship $\log(\text{Stellar Mass} / \text{SMBH Mass})$, and that 23% SMBHs are of matter (located in antimatter galaxies), measuring a value of $(2.290 \pm 5.6\%)$ for the logarithmic relationship $\log(\text{Stellar Mass} / \text{SMBH Mass})$. Thus, two relationships were obtained that are nearly equal to the expected theoretical value (with a final error of less than 1.0%), something that is likely not a mere coincidence. A metrological analysis of the results indicates the practical validity of the used model and also highlights the fact that the mass measurement errors reported by astronomers are very precise, with only 3 cases showing actual measurement errors (as pointed out by the theoretical model) above the predicted range. This result is highly significant as it suggests that the models predicted in the Ulianov Theory are capable of generating new predictions, as in the case of this model, which originates from a cold and empty universe and defines the process of galaxy mass generation through the growth of SMBHs that extract energy from cosmic inflation, transforming it into particles of matter and antimatter in a model coined "Small Bang" by the authors.

1 - Introduction

Antimatter [1] is a form of matter composed of antiparticles that possess properties opposite to those of regular matter particles. For instance, the antiproton has an opposite charge compared to a proton, and the positron (the antiparticle of the electron) carries a positive charge.

When a particle of matter encounters its corresponding antiparticle, they annihilate [2] each other, resulting in a complete conversion of matter into energy, following the equation $E=mc^2$. As a result, the original mass (the sum of the masses of the two particles) transforms into energy in the form of electromagnetic radiation.

The enigma of antimatter [3] arises from the fact that, according to the theories of physics, the Big Bang (the event that gave rise to the universe) should have produced equal amounts of matter and antimatter. However, when we observe the current universe, we find a significant predominance of matter (M) compared to antimatter (AM). This is evident in the widespread absence of large-scale particle-antiparticle annihilations (which would generate significant energy and be easily observable) that should have occurred if planets, stars, or even galaxies of both types, M/AM, were to collide.

The currently accepted answer to this enigma involves the idea of M/AM asymmetry [4], also known as "CP violation." The acronym "CP" refers to "charge-parity" and is linked to the properties of charge (C) and parity (P) inversion. Experimental studies have suggested that there might be small differences in the interactions between particles and antiparticles, indicating that subtle and not yet fully understood physical processes might favor the creation of matter over antimatter in certain situations that could have occurred during the Big Bang.

However, the authors of this paper believe that CP violation alone cannot explain the absence of antimatter or adequately elucidate the origin of matter and the formation of spiral galaxies as observed in our universe. As an alternative to the CP violation model, a new model has been developed to describe the origin and development of our universe. This model is known as the "Small Bang" [14] and is part of a larger Unified Theory developed by P. Y. Ulianov [17][21][23] over 30 years, known as the Ulianov Theory (UT).

The Small Bang model will be briefly described below, but more detailed information can be found in references [15][16]. In the Small Bang universe creation model, everything begins in an exceedingly small space (with the size of a Planck length), void of energy (temperature at absolute zero). This initial universe expands as a 5D space-time (three spatial dimensions and two complex time dimensions) at a velocity slightly greater than the speed of light ($2\pi c$).

After some time, this expanded space, still cold and empty, sees the formation of various types of virtual particle pairs. The pair with the highest energy consists of two micro black holes (uBHs), one composed of matter and the other of antimatter, oscillating in quantum fluctuations of the vacuum, emerging in an infinitesimal time (Planck time), only to annihilate each other immediately after.

During the phase of "cosmic inflation," which is also considered in the Small Bang model (but occurs only in "imaginary time"), the accelerated expansion of space "breaks" some virtual Matter uBH and Antimatter uBH (MuBH / AMuBH) pairs apart, causing them to move away from each other at a speed greater than that of light and so isolating them. The event horizon radii of a uBH also grow during cosmic inflation and increase exponentially, causing the uBH's mass to grow, absorbing mass (AM or M mass) from the empty space, and expel mass (M or AM mass). This expelled matter is propelled at high speeds along the "equatorial" line of the uBH, that is determined by its rotation.

In this model, continuous streams of matter formed by protons and electrons in equal proportions (to maintain a total neutral electric charge) are expelled by an AMuBH, while it "consumes" positrons and antiprotons (that were their virtual pairs and become real ones), in order to exponentially increase its event horizon radius, being "stretched" by cosmic inflation. In analogy, an expanding AMuBH will be an AMBH and behaves like a rotating hose expelling continuous water jets in opposite directions, forming water lines in the shape of a double spiral.

In the Small Bang model, this is the basis for the formation of all matter galaxies and explains where antimatter went (into the ASMBH) and why we don't observe astronomical evidence of energy release from matter-antimatter annihilation. This is because antimatter is "trapped" within the supermassive black holes that exist within each matter galaxy and thus never collides with ordinary matter.

2 – The Formation of Galaxies in the Small Bang

The Small Bang model posits that micro Black Holes (uBHs) initiate with a mass equivalent to the Planck mass and an event horizon radius matching the Planck length. As virtual particle pairs, uBHs (comprising one of matter and one of antimatter) undergo oscillations, spontaneously emerging within quantum vacuum fluctuations, guided by the uncertainties of quantum mechanics' principles. These virtual particles swiftly annihilate in an infinitesimally brief duration, occurring within a few Planck times interval. This annihilation results in a net energy of zero and momentary fluctuations of both "positive energy" and "negative energy".

In this new model, the 3D space is envisioned as an empty bubble, initially starting with a radius equal to a Planck length. Over the span of billions of Planck times, an accelerated expansion of the universe, known as cosmic inflation, takes place. Originally defined within the framework of the Big Bang theory, this process finds application in the Small Bang model as well. During this cosmic inflation phase, numerous isolated virtual pairs of AMuBH (Antimatter micro Black Holes) and MuBH (Matter micro Black Holes) particles are 'cut' due to the space's rapid expansion. These pairs, which once would have annihilated, are now prevented from doing so by the accelerating expansion of space. As a result, they transform into two real uBHs, one being a MuBH and the other an AMuBH. These uBHs undergo exponential growth of their event horizon radii.

The collective inflation rate, across the entire expanse of space, constituting the universe itself, reaches several hundred times the speed of light. At the conclusion of this process, an AMuBH evolves into an ASMBH (Antimatter Supermassive Black Hole), catalyzing the formation of a spiral galaxy. This galaxy is composed of matter expelled during the expansion of the AMuBHs.

This process seemingly challenges the law of conservation of energy by seemingly generating matter and energy from empty space. However, the phenomenon of cosmic inflation itself encompasses what can be termed as "Potential Inflation of Space-Time Energy" (PISTE), a substantial energy reservoir. A minor fraction of PISTE impacts the virtual micro Black Holes pairs, transforming them into M/AM uBHs (matter and antimatter uBHs) components in equal proportions, without transgressing the "CP" (Charge-Parity) symmetry. This transformative process gives rise to the creation of all observed galaxies within our current universe. Initially, each virtual uBH distinctively distances itself from its corresponding "anti-particle," subsequently progressing to evolve into a regular Black Hole (BH). Eventually, driven by the utilization of PISTE energy, these BHs experience exponential growth, culminating in their transformation into Supermassive Black Holes (SMBHs). This intricate energy process concurrently contributes to the generation of their own mass and facilitates the formation of the spiral galaxies surrounding them.

Within the framework of the Ulianov Theory, a conjecture asserts that matter repels antimatter. In this hypothesis, a rotating Antimatter Black Hole (AMBH) engenders growth through the selective interaction with virtual M-AM (Matter-Antimatter) particle pairs, such as protons-antiprotons and electrons-positrons, at the periphery of its event horizon. Consequently, the BH's event horizon acts as a division point for these virtual pairs, permitting the absorption of antimatter particles and expelling matter particles at velocities of remarkable magnitude. This dual process imparts an accelerated rotation to the black hole, either clockwise or counterclockwise, while simultaneously discharging matter particles at extraordinary speeds in divergent jets. Intriguingly, this dynamic equilibrium maintains the collective angular and linear momentum of the entire system, encompassing both the galaxy and the Supermassive Black Hole (SMBH), at an equilibrium of zero.

The expulsion of particles at such elevated velocities is a phenomenon localized solely along the "equatorial line" of the rotating black hole. This spatial restriction ensures that the matter particles can circumvent the gravitational influence of the BH, ultimately escaping its grasp. On the other hand,

matter particles generated within regions akin to the poles of the BH, characterized by an absence of the necessary escape velocity, converge upon the event horizon. In a paradoxical interaction, these incoming matter particles annihilate the antimatter particles ingested during earlier stages, thereby contributing to the black hole's complex dynamics.

Despite the Uljanov Theory's assertion of matter's repulsion from antimatter, it's important to acknowledge that according to Einstein's General Theory of Relativity, the initial spacetime distortion induced by matter mirrors that engendered by an equivalent mass of antimatter. This equivalence arises due to the intrinsic characteristics of curved spacetime, where traditional elliptical orbits (often attributed to planets circling stars) yield to the principle of geodesic paths. This occurrence mimics the motion of an object traversing a straight trajectory within the context of curved space. As such, the trajectory of a planet encircling a matter-based star exhibits similarities to that of a planet orbiting an antimatter-based star, under the condition that identical masses are sustained.

Consequently, this equivalence leads to an intriguing proposition: Deducing whether a celestial body, be it a star or a black hole, is composed of matter or antimatter solely through the analysis of astronomical orbits becomes a formidable task. The dual behavior stemming from the mutual impact of matter and antimatter engenders orbits that share astonishing resemblances, rendering the classification of a cosmic entity as matter or antimatter an intricate challenge.

In the context of the Small Bang model, two questions emerge when focusing on the evolution of solely antimatter supermassive black holes (ASMBHs) in the formation of matter galaxies within our universe:

- A. What becomes of the micro black hole of matter that initially arises alongside the micro black hole of antimatter?
- B. Given that the tally of matter particles (namely protons and electrons) expelled by the ASMBH corresponds to the quantity of antimatter particles (antiprotons and positrons) "absorbed" by the black hole, an intriguing paradox surfaces: Why does the mass of the ASMBH not align with the mass of the galaxy it ultimately gives rise to?

The response to question (A) considers that in the Small Bang scenario, the growth rate of an AMuBH (antimatter uBH), in terms of the number of particles absorbed by the uBH, is significantly greater than that of a MuBH (matter Ubh). Consequently, collisions will occur between M/AM uBHs in the early universe, leading to the elimination of all nearby MuBHs situated around some AMuBHs. The remaining MuBHs will mutually attract each other while simultaneously repelling AMuBHs, forming isolated clusters. As this process unfolds, these clusters will eventually generate clusters of antimatter galaxies. These antimatter galaxy clusters will be separated from matter galaxy clusters by distances of hundreds (or thousands) of millions of light-years, preventing further collisions. Thus, collisions between matter and antimatter galaxies cannot currently take place.

The response to question (B) calls for a more detailed examination of the Uljanov Theory within the context of the Small Bang model, which yields a significant and experimentally testable prediction:

- $\text{Log}(\text{Mass of matter galaxy} / \text{Mass ASMBH}) = 2.963;$
- $\text{Log}(\text{Mass of antimatter galaxy} / \text{Mass SMBH}) = 2.317.$

The derivation of these theoretical values will be explained in section 4 of this article, followed by an analysis of astronomical data, in section 5, concerning 100 supermassive black holes (SMBHs), where 77 are composed of antimatter and 23 are associated with antimatter galaxies.

3 – Current State of Research on SMBH

The relationship between the masses of galaxies and the supermassive black holes (SMBHs) at their cores is a dynamic field of research in astrophysics and cosmology [5][6][11]. A well-established empirical correlation, known as the "M-sigma relation," underpins this investigation, linking the mass of a central SMBH with the velocity dispersion of stars within the galaxy's bulge. This correlation suggests an intrinsic connection between the growth of SMBHs and the formation and evolution of their host galaxies.

Astronomers Marconi and Hunt [8] introduced the M-sigma relation in 2003, named after the mass of the black hole (M) and the velocity dispersion ($\sigma = \text{sigma}$) of stars in the galaxy's bulge. The M-sigma relation is often expressed as a power-law equation:

$$\log(\text{MBH}) = \alpha + \beta * \log(\sigma)$$

where:

MBH represents the mass of the SMBH.

σ is the velocity dispersion sigma of stars in the bulge.

α and β denote coefficients dependent on the galaxy sample and measurement methodology.

The numerical values within the M-sigma relation can vary based on the studied galaxy and SMBH sample [13]. However, there's a consistent trend where larger galaxies tend to possess more massive central black holes. The correlation's scatter is substantial, hinting at the potential influence of additional factors.

Key aspects regarding supermassive black holes [12] and lingering inquiries concerning their nature and origin include:

- Supermassive black holes are typically found at the centers of large galaxies.
- The time elapsed since the Big Bang is inadequate for black holes to reach billions of solar masses solely through accretion.
- Ancient quasars, exceptionally luminous celestial objects, are likely powered by supermassive black holes present since the early universe.
- Beyond their energy output, the connection between supermassive black holes and galaxy formation, as well as the broader universe's structure, is captivating.
- Intermediate-mass black holes might have emerged in the early universe from collapsing gas clouds or star collisions, potentially growing into supermassive scales through successive collisions and accretion. However, challenges arise due to the early universe's high temperature conditions and accretion rate limitations.
- Existing explanations for supermassive black hole formation possess constraints, yielding various rival theories involving dynamic processes and primordial black holes.
- The true origin of supermassive black holes remains enigmatic, with fundamental gaps in our comprehension.
- Galaxy mass and the central supermassive black hole's mass are correlated, yet the underlying nature of this link remains partly elusive.
- Mergers among supermassive black holes are theoretically plausible but encounter obstacles due to black hole dynamics and the "final parsec problem," where orbital decay occurs too gradually for mergers to transpire within the universe's age. Certain supermassive black holes, like those in pristine spiral galaxies, defy explanations via collisions with other galaxies, hinting at alternative formation mechanisms.
- The universe's age doesn't afford black holes the time required to evolve into supermassive dimensions solely through accretion.

- In spite of progress, considerable aspects concerning supermassive black holes are still unknown, with scientists anticipating unforeseen discoveries to reshape understanding.

To conclude this discussion on the significance of SMBH research, let us reflect on the perspective of eminent scientist Dr. M. Volonteri [5], who articulated [12] the following assertion:

"Supermassive black holes interest scientists for more than just their energy efficiency. Their formation and evolution are clearly connected to the development of galaxies, and to the even larger story of our entire Universe's history and structure. Solving the mystery of these cosmic giants would represent a significant step in scientists' ongoing effort to understand why things are the way they are. There are also theories about 'primordial black holes', which could have come into existence and begun growing before there were stars. But this is completely unknown territory. We don't have any observational proof to test this principle."

4 – Calculation of SMBH-Galaxie Mass Relations

Within the framework of the Ulianov Theory (UT), both a proton and an electron are represented as one-dimensional strings, each possessing an equal length Li (determined by the length of the imaginary time axis multiplied by the speed of light). As the collapse of imaginary time unfolds (from the viewpoint of an observer experiencing real time), these strings coil into distinct spherical membranes, harboring mass and electric charge either on their surfaces or within their volumes. Each string can be compacted (or wound) into a membrane in four distinct modes:

- 1D Mode: Strings wound around a 1D circular line with unit thickness (Planck length). This mode applies to photon membranes.
- 2D Mode: Strings wound around a 2D spherical surface with unit thickness (Planck length). This mode pertains to electron and positron membranes.
- 2.5D Mode: Strings wound around a 2D spherical surface with thickness $H PL$. This mode applies to muon electron membranes.
- 3D Mode: Strings wound around a 3D spherical volume. This mode corresponds to proton and antiproton membranes, as well as tau electron membranes.

In UT, the membrane masses are conceptualized as nano black holes (nBHs), characterized by unit masses significantly smaller than the Planck mass. Consequently, the event horizon of nBH remains inaccessible (smaller than a Planck length) unless a substantial number of nBHs aggregate in a confined space, thereby forming a black hole. The number of nBHs within a given membrane is defined by Li divided by the average length of the wound membrane (typically determined by the radius of the membrane multiplied by 2π).

For instance, concerning the proton, this model allows the establishment of an inversely proportional relationship between the radius of the proton membrane (which manifests as a solid sphere) and its mass through the following expression:

$$m_{prot} = \frac{2h}{\pi c r_{prot}} \quad (1)$$

Likewise, for the muon electron case, UT models facilitate the formulation of the following relation:

$$m_{muon} = m_{elec} \pi \sqrt{\frac{3\pi m_{prot}}{4 m_{elec}}} \quad (2)$$

In the Small Bang model, the behavior of black holes (BHs) differs according to their composition,—antimatter BHs (AMBHs) and matter BHs (MBHs), and how they interact with falling particles.

For AMBHs, only the 2D mode is accepted for all particles that fall within them. Consequently, when an antiproton enters an AMBH, the usual 3D packing of the antiproton is forbidden by the AMBH. As a result, the antiproton transitions from a 3D volume to a 2D surface, causing its mass to reduce to the value of a positron's mass (which equals that of an electron).

Conversely, MBHs accept only the 2.5D mode. Thus, when a proton falls into an MBH, its typical 3D packing converts to a 2.5D packing, causing a reduction in its observed mass. Similarly, when an electron falls into an MBH, its normal 2D packing transforms into a 2.5D packing, leading to an increase in its observed mass within the MBH, which becomes equivalent to the reduced proton mass. This occurs since both particles are confined to the 2.5D surface, which is the only available mode within the MBH.

In this “mass changing” model, the "mass energy" lost by the antiproton or proton upon falling into a BH is conserved by accelerating the BH's rotational speed. This, in turn, stores the "mass energy" as an increase in the BH's angular momentum energy, without resulting in rising of the BH's mass by the total mass of the antiproton or proton that fell in it. Importantly, the angular momentum of a BH is relative to the spacetime structure itself. Consequently, the total mass energy "liberated" by antiprotons or protons within the BH, enhances the rotation of both the BH and the galaxy formed around it.

The authors believes that this phenomenon, which may currently be related to a type of "dark matter" effect, contributes to galaxies rotating at higher speeds than anticipated. For instance, the ASMBH in the Milky Way's center, exhibits heightened angular momentum, generating elevated rotational speeds for the galaxy. This leads to the notion of "invisible matter" or dark matter around the Milky Way, causing it to rotate faster than predicted only by our galaxy “luminous mass”.

The Ulianov Theory posits that all AMBHs at the centers of the matter galaxies, convert 99.9% of their original "protons mass energy" into rotational kinetic energy, accelerating their angular velocity to a value 30,30 times greater than a normal value. This acceleration, in turn, propels the galaxy itself to rotate at a higher angular velocity in the opposite direction, creating the illusion of the galaxy's mass being 5.51 times greater than actual. Similarly, the UT proposes that an MBH at the center of an antimatter galaxy, converts 99.5% of its mass energy, into rotational kinetic energy, amplifying its angular velocity to a value 13,88 times greater. This causes the antimatter galaxy itself to rotate at an increased angular velocity in the opposite direction, fostering the impression that the galaxy's mass is 3.73 times greater than observed. Thus, differentiating an antimatter galaxy could potentially involve assessing the estimated amount of “dark matter” for each galaxy, with matter galaxies potentially displaying "dark matter" around 5.6 times the galaxy's mass, and antimatter galaxies around 3.7 times.

In the Small Bang model, the relationship between the mass of an antimatter SMBH and the mass of the matter galaxy it generates, can be deduced from the particles generated at the event horizon of the rotating antimatter SMBH, during cosmic inflation. Antimatter particles are utilized by the ASMBH to exponentially increase its horizon event radius, while matter particles are expelled to form the surrounding galaxy. The equivalence of total electric charge between an ASMBH and the galaxy signifies that, the same number (N) of proton-antiproton and electron-positron pairs are generated, during cosmic inflation.

Given N antiprotons and N positrons being "consumed" by the ASMBH, and N protons and N electrons, being expelled in opposing high-speed jets along a spiral trajectory that shapes the entire galaxy. So, the relationship between the galaxy and the ASMBH's mass can be defined as:

Mass of matter Galaxy:

$$\begin{aligned} M_{\text{stellar}} &= N (m_p + m_e) \\ M_{\text{stellar}} &= N (Rm_{pe} m_e + m_e) \\ M_{\text{stellar}} &= N m_e (Rm_{pe} + 1) \end{aligned} \quad (3)$$

Mass of ASMBH:

$$\begin{aligned} M_{\text{ASMBH}} &= N (2D[m_p] + m_e) \\ \text{where } 2D[m_p] &= m_e \\ M_{\text{ASMBH}} &= 2 N m_e \end{aligned} \quad (4)$$

By applying Equation (4) to Equation (3):

$$\begin{aligned} M_{\text{stellar}} / M_{\text{ASMBH}} &= N m_e (Rm_{pe} + 1) / (2 N m_e) \\ M_{\text{stellar}} / M_{\text{ASMBH}} &= (Rm_{pe} + 1) / 2 \end{aligned} \quad (5)$$

$$M_{\text{stellar}} / M_{\text{ASMBH}} = 918.5$$

$$\log (M_{\text{stellar}} / M_{\text{ASMBH}}) = 2.963 \approx 3 \quad (6)$$

$$M_{\text{stellar}} \approx 1000 M_{\text{ASMBH}}$$

Thus, the model suggests that the mass of an antimatter SMBH will be approximately 0.1% of the mass of the galaxy that it created.

For a matter SMBH, a similar process unfolds, generating N proton-antiproton and electron-positron pairs during cosmic inflation. N antiprotons and N positrons are expelled by the SMBH, contributing to the creation of an antimatter galaxy. Conversely, N protons and N electrons are "consumed" by the SMBH to expand its event horizon. As particles enter the SMBH, the proton's winding factor shifts to mode 2.5D, leading to a mass reduction of the mode 3D mass of the proton, expressed as mode 2.5D[m_p]. This reduction is calculated using the formula: $m_p = m_e \sqrt{Rm_{pe}}$.

However, an additional factor of 3^2 , related to the winding of proton strings around three types of (Ulianov Holes) uholes (similar to the normal formation of a proton through three types of quarks), results in 2.5D[m_p]: $m_p = \frac{m_e}{9} \sqrt{Rm_{pe}}$. Additionally, the electron undergoes a transition from 2D winding to 2.5D, and its mass within the matter BH, increases and becomes equal to that of the proton (inside the MBH), i.e., 2.5D[m_e] = 2.5D[m_p]: $m_p = \frac{m_e}{9} \sqrt{Rm_{pe}}$.

In this context, the relationship between the antimatter galaxy's mass and the matter SMBH mass can be defined as follows:

Mass of antimatter Galaxy:

$$\begin{aligned} M_{\text{stellar}} &= N (m_p + m_e) \\ M_{\text{stellar}} &= N (Rm_{pe} m_e + m_e) \\ M_{\text{stellar}} &= N m_e (Rm_{pe} + 1) \end{aligned} \quad (7)$$

Mass of matter SMBH:

$$M_{\text{SMBH}} = N (2.5D[m_p] + 2.5D[m_e])$$

where $2.5D[m_e] = 2.5D[m_p] = \frac{m_e}{9} \sqrt{Rm_{pe}}$.

$$M_{\text{SMBH}} = 2N \frac{m_e}{9} \sqrt{Rm_{pe}} \quad (8)$$

Applying Equation (7) to Equation (7):

$$\begin{aligned} M_{\text{stellar}} / M_{\text{SMBH}} &= \frac{N m_e (Rm_{pe} + 1)}{2N \frac{m_e}{9} \sqrt{Rm_{pe}}} \\ M_{\text{stellar}} / M_{\text{SMBH}} &= \frac{9 (Rm_{pe} + 1)}{2\sqrt{Rm_{pe}}} \end{aligned} \quad (9)$$

$$M_{\text{stellar}} / M_{\text{SMBH}} = 192.924$$

$$\log (M_{\text{stellar}} / M_{\text{SMBH}}) = 2.285 \quad (10)$$

Thus, according to this model, the mass of a matter SMBH will be approximately 0.5% of the mass of the antimatter galaxy that it created.

The calculations presented are founded on the Small Bang model [14], and the relationships derived within the Ulianov Theory's fundamental particles model [21], and withing Ulianov Theory's strings models [17].

5 - Observation of SMBH-Galaxy Masses in Astronomical Databases

In this section, the focus shifts to the observation of astronomical data related to SMBHs. Numerous databases offer recorded mass values for both SMBHs and their host galaxies. If the theoretically predicted relationship between these two masses, as suggested by the Small Bang model and presented in equation (6), were a fixed factor of 1000, astronomers would likely have noticed this correlation long ago. However, in the absence of such a direct relationship, astronomers have established alternative connections, such as the M-sigma factor discussed in Section 3.

In the context of this topic, an examination of articles like [7] reveals tables containing observed and calculated mass values for SMBHs and their associated galaxies. In the provided article, authored by H. Suh et al., the selection of their sample of 100 MBHs is described as follows:

"We investigate the cosmic evolution of the ratio between black hole (BH) mass (MBH) and host galaxy total stellar mass (Mstellar) out to $z \sim 2.5$ for a sample of 100 X-ray-selected moderate-luminosity, broad-line active galactic nuclei (AGNs) in the Chandra-COSMOS Legacy Survey... We obtain 100 broad-line AGNs covering the redshift range $z = 0-2.5$."

The table from Dr. Suh's research consists of 100 rows, each containing the following information:

- Column A: Object ID - Identification of the object.
- Column B: Redshift - Redshift of the spectral lines.
- Column C: log MBH - Logarithm of the SMBH mass in terms of solar mass (M_{\odot}) derived using the virial method. Values are provided with two decimal places and a single associated error range (\pm error).
- Column D: log Lbol - Logarithm of AGN bolometric luminosity.
- Column E: log Mstellar - Logarithm of the total stellar mass in terms of solar mass (M_{\odot}) derived from SED fitting. Values are provided with two decimal places and an error range [-error, +error].
- Column F: Instrument - Instrument used for spectroscopy.
- Column H: Line - Broad emission line utilized.

The authors then obtained these astronomical data table from [7], appending an additional initial column with line numbers to assign a unique point number to each SMBH and its corresponding galaxy. The complete dataset, the calculations and analysis, made by the authors, and all graphics presented here, can be accessed in a excel table available at [34].

Table 1 illustrates an example of the utilized data, with three points highlighted in red to indicate potential issues in the reported errors theoretical mass errors.

Table 1: selection of lines illustrating the complete used data table presented in[7]. Three points highlighted in red point out instances where reported errors in the table might have posed issues.

Line Num.	Object ID	Redshift	log Lbol	log MBH		log Mstellar			Instrument	Line
				Value	\pm error	Value	- error	+error		
1	cid_36	1.826	45.63	9.38	0.06	12.18	0.04	0	DEIMOS	Mg II
2	cid_61	1.478	45.38	8.62	0	11.48	0.15	0	DEIMOS	Mg II
3	cid_66	1.512	45.77	8.45	0.03	11.21	0.01	0.24	DEIMOS	Mg II
12	cid_142	0.699	45.5	8.43	0.16	11.25	2.84	0	DEIMOS	H β
21	cid_358	0.372	45.61	8.32	0.11	10.66	1.17	0	DEIMOS	H α
24	cid_175	1.627	45.51	8.47	0.77	11.09	0.03	0.18	DEIMOS	Mg II
30	cid_481	2.283	45.68	8.72	0.01	11.22	0.06	0.12	DEIMOS	Mg II
34	cid_512	1.516	45.98	8.41	0.06	11.99	0.09	0.06	FMOS	H α
41	cid_566	1.458	45.84	8.87	0.1	10.99	0.38	0.06	DEIMOS	Mg II
62	cid_1174	0.088	45.58	5.85	0.01	8.01	0	0	DEIMOS	H α
69	cid_2564	2.01	45.29	8.47	0.07	11.02	0.02	0.03	DEIMOS	Mg II
76	lid_338	1.209	45.83	8.06	0.01	11.57	0.23	0	DEIMOS	Mg II
95	lid_1538	1.523	46.03	8.19	0.05	11.84	0.06	0.06	FMOS	H α
99	lid_1878	1.608	45.69	8.9	0.02	11.67	0.04	0	FMOS	H α
100	lid_3456	2.146	45.03	8.02	0.57	11.87	0.06	0	DEIMOS	Mg II

Figure 1(a) presents a plot with points defined by the logarithm of the galaxy's mass (log Mstellar) against the logarithm of the MBH's mass (log MBH). The orange dashed line represents the theoretically expected relationship ($\log \text{MBH} = \log \text{Mstellar} - 2.963$), while the blue line signifies the relationship derived from linear interpolation of the 100 points. The interpolation yields the equation ($\log \text{MBH} = 0.672 \log \text{Mstellar} + 0.9142$), which significantly diverges from the expected theoretical value.

Figure 1(b) depicts a plot featuring 100 values for the ratio ($\log(\text{M}_{\text{stellar}} / \text{MBH})$). In theory, this plot should manifest as a straight line of points situated at the y-coordinate of 3.0. However, instead of this anticipated linearity, scattered points are observed within a range spanning from 1.5 to 3.8. This observation indicates a variable ($\text{M}_{\text{stellar}} / \text{MBH}$) ratio spanning from 32 to 6300, an approximately 200-fold variation. This is in contrast to the predicted fixed ratio of 2.964 given by equation (6).

Upon examining the graphs in Figure 1, it becomes apparent that the theoretical relationships proposed by the Ulianov Theory, and Small Bang models, between galaxy mass and SMBH mass are not reflected in actual astronomical data.

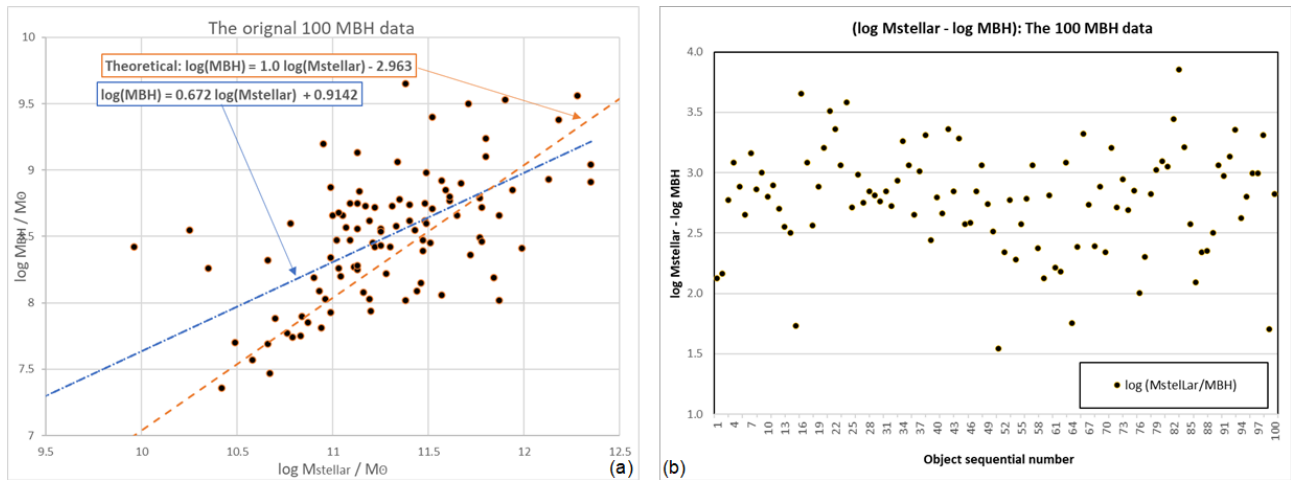


Figure 1 – a) Graph illustrating a logarithmic plane, depicting the mass of each SMBH in relation to the mass of its respective galaxy; b) Logarithm of the ratio ($\text{M}_{\text{stellar}} / \text{MBH}$).

However, before dismissing the Small Bang model, it's crucial to acknowledge the existence of both highly accurate and less accurate mass values within the dataset of 100 points representing SMBH mass and galaxy mass. Some of these values exhibit remarkably low mass total errors, measuring less than 0.1. Conversely, there are instances of larger error values, such as those highlighted in Table 1 for points 24, 21, and 12. These points have corresponding maximum errors of 0.77, 1.17, and a substantial 2.84, rendering them significantly erroneous and practically invalidating their inclusion in the graphs and calculations. To account for these theoretical mass measurement errors introduced by optical instruments (referred to as mass errors), an analysis of the logarithm-subtracted graph was conducted. The goal was to estimate a theoretical maximum mass measurement error for each data point. This generates a $\log(\text{mass})$ total error, associated with the $\log(\text{mass})$ subtraction:

$$\log(\text{M}_{\text{stellar}}/\text{MBH}) = \log(\text{M}_{\text{stellar}}) - \log(\text{MBH}) \quad (11)$$

The calculation of the mass total error was a straightforward process, involving the addition of errors attributed to $\log(\text{MBH})$ mass (\pm error from Table 1) and the average error associated with $\log(\text{M}_{\text{stellar}})$ mass (+error and -error from Table 1) for all 100 points in the dataset. Once this estimated mass total error was determined, the complete set of data points was reorganized in ascending order based on this total error. This reorganization led to a new visual representation of the points on the graph in Figure 1(b), which is presented in this revised arrangement in Figure 2(a).

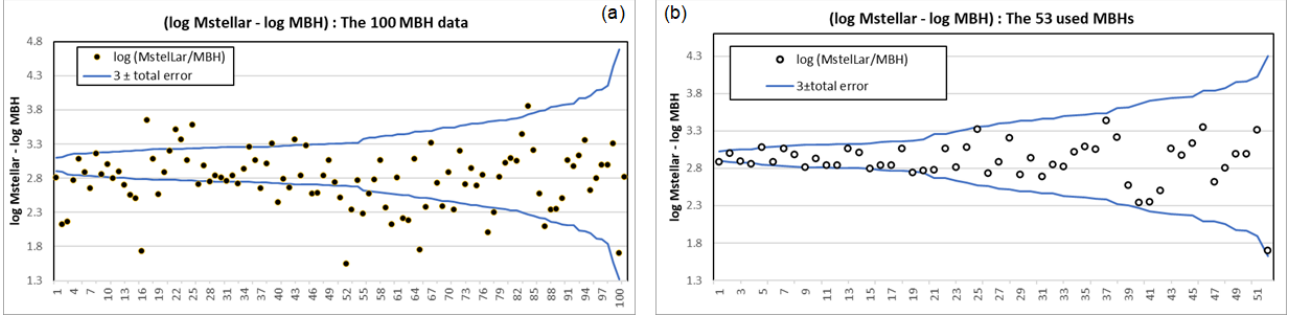


Figure 2 – a) Graph depicting the logarithm of the ratio (M_{stellar} / MBH) with points ordered based on the maximum total error in each measurement. b) Same graph with only 53 points selected within the range of $3 \pm \text{total error}$.

Upon conducting this analysis of the reorganized data, two distinct groups of points become apparent: the first group includes 54 points (used MBH points) falling within the range defined by the blue lines ($3 + \text{total error}$ and $3 - \text{total error}$) as depicted in Figure 2(b), while the second group consists of 47 points (unused MBH points), lying outside this range, as illustrated in Figure 3(a).

Within the blue range, the used points, consistently converge towards a value near 3.00, with random errors falling within the $\pm \text{total error}$ range. This suggests that ideally, all 54 used points within this range should converge to the theoretical value of 2.963, deviating from it due to random measurement errors. As the actual relation between galaxy mass and SMBH mass can be expressed as $\log(M_{\text{stellar}}/MBH) = 2.963$, a new concept of measurement error can be introduced to this dataset. For each Antimatter SMBH point (pt), this measurement error can be calculated using the formula:

$$\text{Measurement error[pt]} = 2.964 - \log(M_{\text{stellar}}[\text{pt}]) - \log(MBH[\text{pt}]) \quad (12)$$

Upon closer examination of these newly calculated measurement errors and the total errors associated with the 47 unused points (as shown in Figure 3(b)), it becomes evident that several points exhibit relatively high measurement errors. However, a significant proportion of these 47 points fall within a measurement error limit below (total error + 0.2).

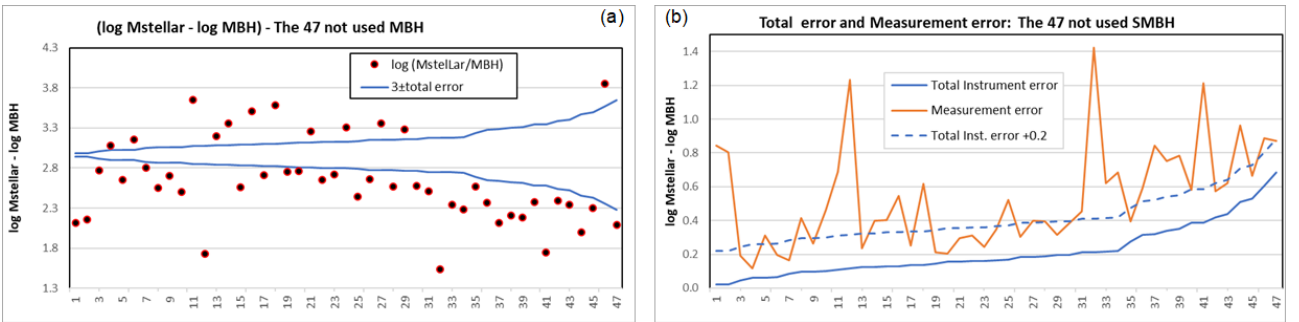


Figure 3 – a) Same graph as in 2(b) with the remaining 47 points selected outside the range of $3 \pm \text{total error}$; b) Graph depicting the total error and theoretical measurement error for the 47 points from Figure 3(a).

This new analysis, has successfully identified 77 points that fall within the range of $2.963 \pm (\text{total error} + 0.2)$, allowing us to classify them as antimatter SMBHs. This classification aligns with the theoretical relation of 2.963, which was calculated in section 4 based on the UT model of ASMBHs behavior.

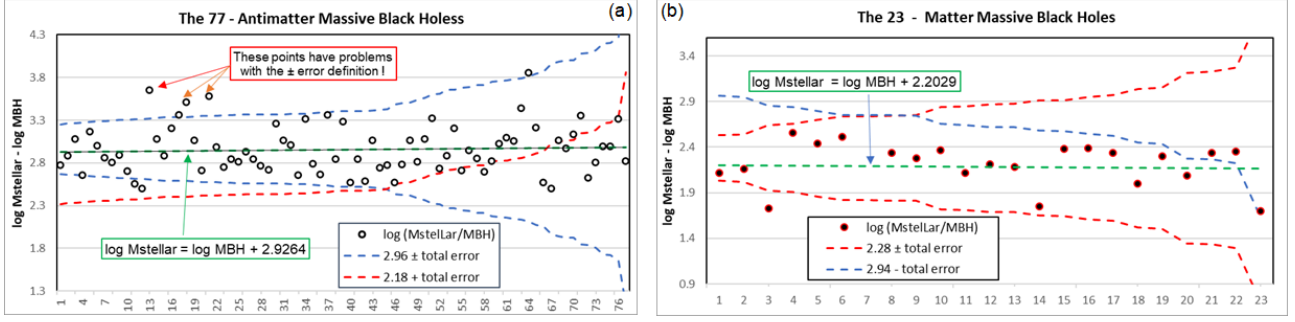


Figure 4 – a) Graph showing the logarithm of the (Mstellar / MBH) ratio with points arranged based on the total theoretical error in each mass measurement, featuring 77 points classified as antimatter SMBHs. b) Same graph as in 4(a) with the remaining 23 points defined as matter SMBHs selected within a range of $2.28 \pm$ total error.

This classification can accurately be applied to 74 of the used points. However, it's worth noting that 3 used points (points 34, 76, and 95 in Table 1, indicated in red to highlight their total errors) displayed mass total errors initially reported as 0.20. Upon recalculating the measurement errors, we found them to be 0.60, three times greater than the theoretical mass total error initially calculated by the astronomers who compiled the 100 MBH data set.

For the remaining 23 unused points, they will be considered as matter SMBHs. As such, a new measurement error for these matter galaxies can be calculated using the formula:

$$\text{Measurement error[pt]} = 2.285 - \log(\text{Mstellar[pt]}) - \log(\text{MBH[pt]}) \quad (13)$$

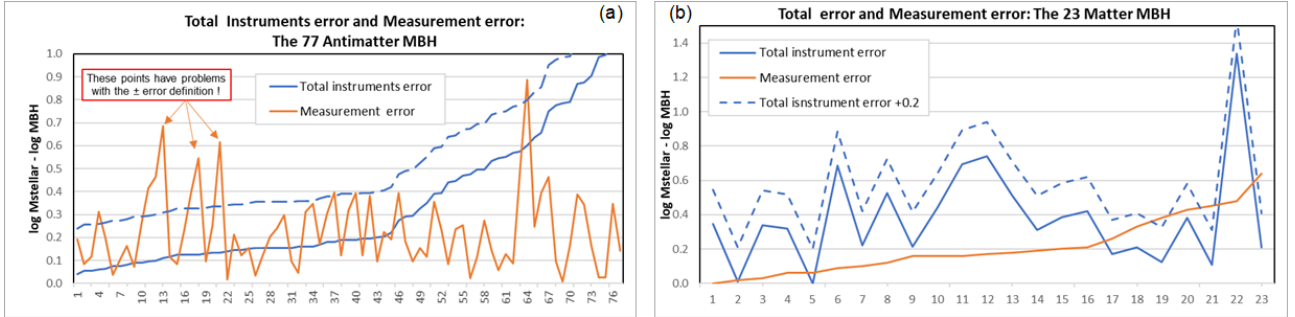


Figure 5 - a) Graph showing the total error and the theoretically defined measurement error for the 77 antimatter SMBHs. b) Same graph as in 5(a), but for the 23 matter SMBHs.

Figures 5(a) and 5(b) depict the new measurement errors alongside the standard mass total errors for all 100 points. These graphics show that a total of 75 points possess measurement errors smaller than the predicted mass total errors. Among them, 22 points fall within the range of [total error to total error + 0.2]. Only three points, as previously mentioned, exhibited discrepancies between the standard mass total error and the new measured mass error.

With this additional error correction, 24 more points can be classified as antimatter SMBHs, generating a total of 77 identified ASMBH, as shown in Figure 5(a), while the remaining 23 points are classified as matter SMBHs placed in antimatter galaxies, as presented in Figure 5(b). Thus, the data table was divided into two groups: a matter galaxies table (MGT) with 77 points and an antimatter galaxies table (AMGT) with 23 points.

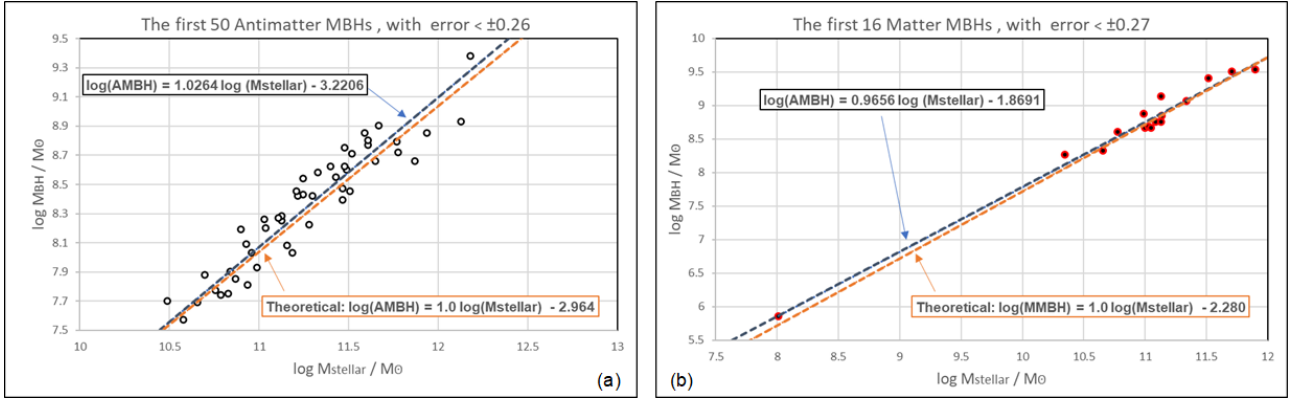


Figure 6 - a) Graph showing a logarithmic plot with the mass of 50 antimatter SMBHs relative to the mass of their host galaxies. Only 50 points from the Antimatter SMBH - Matter Galaxy Table (out of 77 available) were used where the total error is less than ± 0.26 ; b) Graph showing a logarithmic plot with the mass of 16 matter SMBHs relative to the mass of their host galaxies of antimatter. Only 16 points from the Matter SMBH - Antimatter Galaxy Table (out of 23 available) were used, where the total error is less than ± 0.27 .

After excluding 33% of the points with higher mass errors (greater than 0.26) from each table, a total of 66 mass points (50 points in MGT and 16 points in AMGT) were utilized to create the graphs in Figure 6. These graphs reveal that, by separating the SMBHs into two distinct groups and removing the points with higher mass total errors, a nearly perfect correlation between the theoretical orange lines and the interpolated blue lines becomes apparent, as depicted in Figures 6(a) and 6(b).

Finally, Figure 7 visually represents the division between matter and antimatter SMBHs in relation to their relationships with galaxy masses using all 100 data points. The distinction between the theoretical lines (in orange) and the interpolated lines (in blue) is more pronounced here, as the inclusion of high error points contributes to errors in the blue interpolated lines. Moreover, it's clear from the plot that two distinct groupings exist, confirming the division between matter and antimatter galaxies. This observation is further supported by this dataset of 100 points.

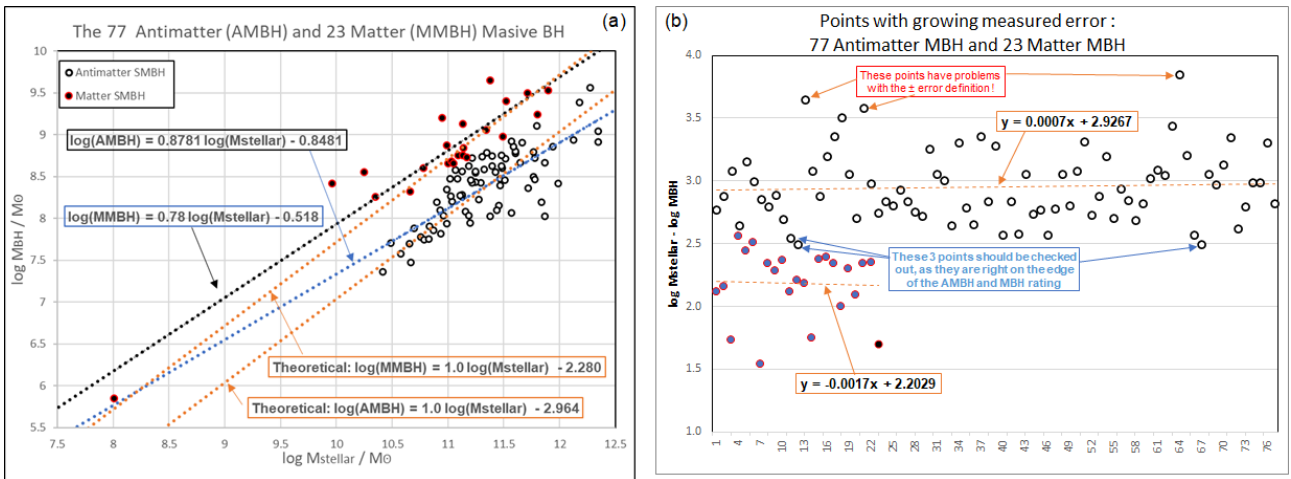


Figure 7 - a) Graph showing a logarithmic plot with the mass of each type of SMBH relative to the mass of its host galaxy; b) Logarithm of the ratio (Mstellar / MBH) for the two types of SMBHs.

In Figure 7(a), it becomes apparent that antimatter galaxies are not only smaller but also less abundant compared to matter galaxies. This observation aligns with the Small Bang hypothesis, suggesting that the growth of matter uBHs is slower, leading to the formation of smaller antimatter galaxies, and that matter uBH have a higher probability of annihilation due to collisions with larger-mass antimatter uBHs. This characteristic is evident in Figure 8, where galaxies are arranged according to their names,

masses and redshifts. Antimatter galaxies are positioned at the lower end, and as the mass increases, about 90% of the galaxies transition to being matter galaxies, in accordance with the predictions of the Small Bang model.

Regarding the mass of matter SMBHs, which are responsible for generating antimatter galaxies, their mass distribution should resemble that of the antimatter galaxies they inhabit. However, despite the slower growth rate of uBHs, the observed mass within them (for the same number of absorbed particles) is five times greater. Consequently, matter SMBHs occupy an intermediate position in the mass ranking, as depicted in Figure 8.

The classification of objects based on names and redshifts provides insight into the proximity of galaxies in angular direction (as similar names usually indicate nearby regions) and distance (matching redshifts). From Figure 8, it can be inferred that antimatter galaxies [cid_399, cid_340, cid_346] are likely part of the same cluster. Given that the analysis involves a sample of only 100 observed galaxies, distributed across a vast spatial volume, it explains the observation of a single cluster of antimatter galaxies. Thus, the present analysis warrants extension to the entire available database, comprising thousands of galaxies, to confirm whether these galaxies are indeed distributed in isolated clusters of the same type, as predicted by the Small Bang model.

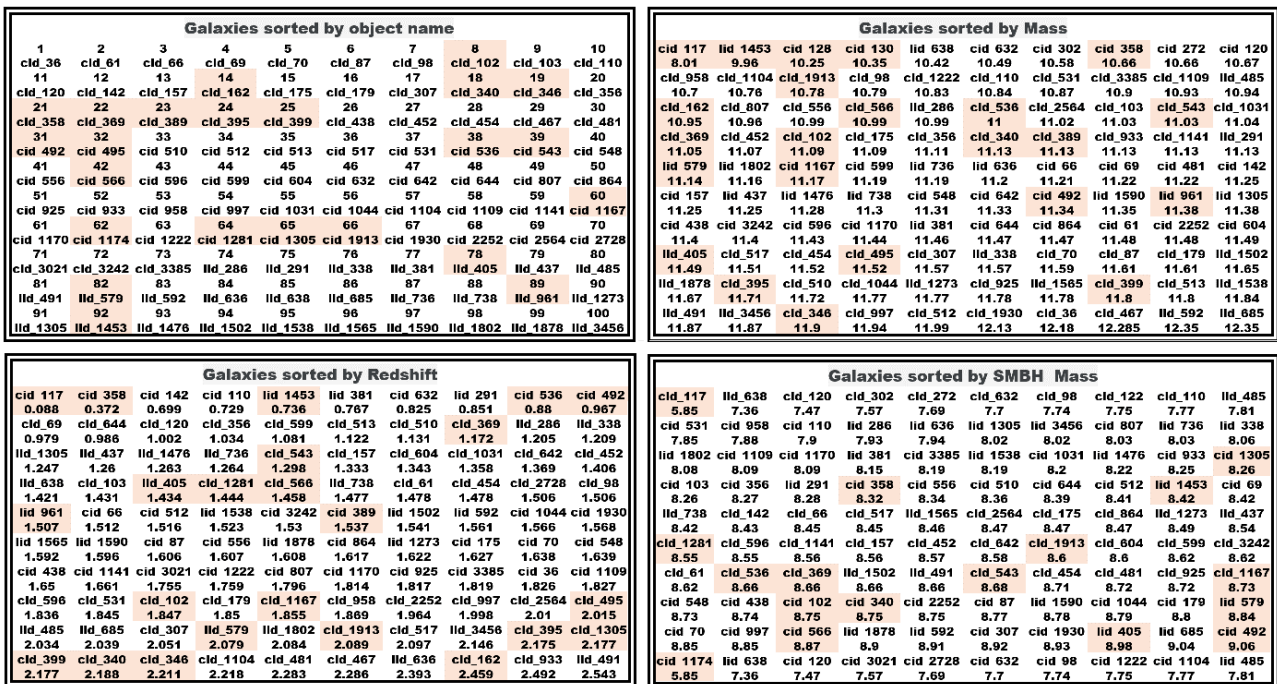


Figure 8 - The 100 galaxies sorted by name, galaxy mass, SMBH mss, and redshift. Galaxies of antimatter have a colored background for the text, while galaxies of matter have a white background for the text.

In these dataset analysis conclusions, these observations lead us to acknowledge that the theoretical relationships proposed by the Ulianov Theory and Small Bang models, for galaxy and SMBH mass are indeed observed in real astronomical data. The data analysis lends support to the Small Bang model's predictions about, the growth of matter and antimatter SMBHs, with distinct characteristics exhibited by both types. However, to validate these findings and assess whether galaxies do indeed

cluster into isolated groups of matter and antimatter galaxies, a more extensive analysis involving a larger dataset is necessary.

6 - Conclusion

In this comprehensive study, we have thoroughly examined the relationships between galaxy masses and supermassive black hole (SMBH) masses, as well as the implications of the Ulianov Theory (UT) equations. Through a meticulous analysis of Figures 5(a) and 5(b), we have discerned that, among the 97 analyzed points, the newly calculated measurement errors, derived from UT equations (12) and (13), consistently equal or surpass the theoretically predicted mass total errors obtained through optical instruments' mass measurement processes. This observation leads us to two pivotal conclusions:

Firstly, the researchers responsible for calculating the optical measurement mass errors in the 100 points mass datasets deserve commendation. In 75% of the reported data points, the calculated random measurement error, grounded in the Small Bang model, closely aligns with the \pm total error range predicted for the optical instruments. Additionally, in 22% of the measurements, the measurement error is only slightly above the predicted mass total error, indicating precise predictions. A mere 3% of cases display a discrepancy between the estimated mass total error and the new measurement error, where these points deviate by a factor of three from the theoretical predictions. Given the complexity of calculating mass errors through optical instruments, considering the propagation of numerous measurement mass errors sources, achieving such high precision for 97% of the estimated errors is remarkable. This is further corroborated by the graphs in Figure 5, where only three problematic points stand out with errors three times higher than theoretically predicted.

Secondly, the proficiency demonstrated, by the astronomers, in calculating optical instrument measurement mass errors, empowers us to assert that the Small Bang model can predict $\log(M_{\text{stellar}}/M_{\text{AMBH}})$ as 2.963 ± 0.001 , for matter galaxies and $\log(M_{\text{stellar}}/M_{\text{MBH}})$ as 2.285 ± 0.001 , for antimatter galaxies, in 97% of the analyzed SMBH cases. Only for three exceptional points (cid_512, lid_338 and lid_1538 objects) should the value of $\log(M_{\text{stellar}}/M_{\text{AMBH}})$ be around 3.58 ± 0.07 . This suggests that these unique galaxies might complicate the measurement of their masses and AMBHs. Re-evaluating the theoretical total error while considering these factors or accounting for mass gains through galaxies collisions is crucial. Additionally, galaxies such as cid_2564, cid_556, and cid_481, though classified as matter galaxies, lie on the boundary between matter and antimatter galaxies, suggesting that their mass total errors require confirmation.

In summary, the growth rate of matter uBHs is five times slower in terms of generated M/AM particles. However, a matter uBH's mass is five times greater for the same N value. Consequently, while both matter and antimatter uBHs undergo equivalent mass growth, matter-formed galaxies possess five times more mass. This leads to the annihilation of matter uBHs upon collision with antimatter uBHs, explaining the observation of 3.3 times more matter galaxies compared to antimatter galaxies.

Although no current astronomical data confirms collisions between matter and antimatter galaxies, the Small Bang theory suggests that antimatter galaxies cluster separately from matter galaxies. Applying the method presented in this work, astronomers can categorize spiral galaxies and determine whether these predictions hold. Moreover, within the Small Bang model, stars within a galaxy are composed of the same mass type, and the type cannot be discerned through astronomical behaviors.

The analysis strongly indicates the existence of two categories of supermassive black holes, influencing the types of galaxies they form. This is evident in Figure 7(a), where points are grouped

by two interpolation lines, showing distinct sets separated by a 0.69 offset. Thus, it's reasonable to hypothesize that one type is matter-based, while the other is antimatter-based.

To validate the Small Bang model, the carried out classification, pointed to an Universe composed of 77% matter galaxies and 33% antimatter galaxies. This model, in future research, must be applied to the entire available database, which is composed of tens of thousands of galaxies. In addition to use the two $\log(M_{\text{stellar}}/M_{\text{BH}})$ relations (2.963 and 2.285) defined to separate a M-AM galaxies, the Ulianov Theory proposes an alternative approach for distinguishing between them, by observing their individual "black matter" ratios. A value close to 5.5 indicates a matter galaxy, while a value close to 3.7 suggests an antimatter galaxy.

While the Ulianov Theory's unconventional nature might pose barriers to acceptance, the empirical validation through error analysis, as well as the prediction of mass relationships, is noteworthy. These equations could revolutionize our understanding of galaxies and their formation processes, urging us to contemplate the concept of a "genuine Big Bang."

Furthermore, since 2016, the Ulianov Theory (UT) has critically exam the functionality of the LIGO experiment [31] [32]. It has raised questions about its effectiveness and proposed an alternative approach for a time interferometer RGW (Real Gravitational Waves) detector [33]. This innovative proposal aims to rectify the issues in the LIGO experiment and enable the LIGO detection of RGWs, marking a significant stride in gravitational wave research.

7 - References

- [1] Dirac, P. A. M. (1930). "A theory of electrons and protons." Proceedings of the Royal Society of London. Series A, Mathematical and Physical Sciences, 126(801), 360-365.
- [2] Griffiths, D. J. (1987). "Introduction to Elementary Particles." Wiley-VCH.
- [3] Thomson, M. (2013). "Modern Particle Physics." Cambridge University Press.
- [4] Sakharov, A. D. (1967). "Violation of CP Invariance, C Asymmetry, and Baryon Asymmetry of the Universe." Soviet Physics Uspekhi, 34(5), 392-393.
- [5] Volonteri, M., Madau, P., & Haardt, F. (2003). "The formation of galaxy stellar cores by the hierarchical merging of supermassive black holes." The Astrophysical Journal, 593(2), 661.
<https://iopscience.iop.org/article/10.1086/376722/pdf>
- [6] Tremmel, M., Governato, F., Volonteri, M., Quinn, T. R., & Pontzen, A. (2018). "Dancing to CHANGA: a self-consistent prediction for close SMBH pair formation time-scales following galaxy mergers". Monthly Notices of the Royal Astronomical Society, 475(4), 4967-4977,
<https://academic.oup.com/mnras/article-pdf/475/4/4967/24062532/sty139.pdf>
- [7] Suh, H., Civano, F., Trakhtenbrot, B., Shankar, F., Hasinger, G., Sanders, D. B., & Allevalo, V. (2020). "No significant evolution of relations between Black hole mass and Galaxy total stellar mass up to $z \sim 2.5$." The Astrophysical Journal, 889(1), 32, <https://iopscience.iop.org/article/10.3847/1538-4357/ab5f5f/pdf>
- [8] Marconi, A., & Hunt, L. K. (2003). "The relation between black hole mass, bulge mass, and near-infrared luminosity". The Astrophysical Journal, 589(1), L21, <https://iopscience.iop.org/article/10.1086/375804/pdf>
- [9] J. A. Regan., T. P. Downes., M. Volonteri., et al, (2018) "Super-Eddington Accretion and Feedback from the First Massive Seed Black Holes", <https://arxiv.org/abs/1811.04953>
- [10] UT News, (2023), "Webb Telescope Detects Most Distant Active Supermassive Black Hole, UT News, <https://news.utexas.edu/2023/07/06/webb-telescope-detects-most-distant-active-supermassive-black-hole/>
- [11] C-H. Lin., K-J Chen., C-Y. Hwang.(2023) "Rapid Growth of Galactic Supermassive Black Holes through Accreting Giant Molecular Clouds during Major Mergers of Their Host Galaxies".
<https://iopscience.iop.org/article/10.3847/1538-4357/acd841>
- [12] Barss, P. (2021). "The mysterious origins of Universe's biggest black holes". BBC future,
<https://www.bbc.com/future/article/20210820-where-did-supermassive-black-holes-come-from>
- [13] S. Batu., A. Das.(2019), "The Mass Function of Supermassive Black Holes in the Direct-collapse Scenario."
<https://iopscience.iop.org/article/10.3847/2041-8213/ab2646>

- [14] Ulianov, P. Y. (2012). "Small Bang Creating a Universe from Nothing." <https://vixra.org/abs/1201.0109>
- [15] Ulianov, P. Y., Freeman, A. G. (2015). "Small Bang Model. A New Model to Explain the Origin of Our Universe." *Global Journal of Physics*, 3(1). <https://vixra.org/abs/1211.0157>
- [16] Freeman A. G., Ulianov P. Y. (2011) "The Small Bang Model - A New Explanation for Dark Matter Based on Antimatter Super Massive Black Holes." <http://vixra.org/abs/1211.0157>
- [17] Ulianov, P. Y. (2010). "Ulianov String Theory A new representation for fundamental particles." *Space*, 1, 1. <https://www.academia.edu/download/89325911/1201.0101v1.pdf>
- [18] Ulianov, P. Y. (2013). "One Clue to the Proton Size Puzzle: The Emergence of the Electron Membrane Paradigm." <https://vixra.org/abs/1302.0026>
- [19] Ulianov, P. Y. (2012) "Explaining the Variation of the Proton Radius in Experiments with Muonic Hydrogen." <https://vixra.org/abs/1201.0099>
- [20] Ulianov, P. Y. (2013) "Rotating the Einstein's light clock, to explain the Witte Effect. A basis to make the LIGO experiment work." <https://vixra.org/abs/1302.0134>
- [21] Ulianov, P. Y. (2010) "Ulianov Sphere Network-A Digital Model for Representation of Non-Euclidean Spaces." <https://vixra.org/abs/1201.0100>
- [22] Ulianov, P. Y. (2012) "Explaining the Variation of the Proton Radius in Experiments with Muonic Hydrogen." <https://vixra.org/abs/1201.0099>
- [23] Ulianov, P. Y. (2012) "A New Digital Complex Model of Time." <https://vixra.org/abs/1201.0102>
- [24] Ulianov, P. Y. (2013) "Spacetime Dipole Waves Pressure and Elemental Particles." <https://vixra.org/abs/1306.0222>
- [25] Ulianov P. Y. (2013) "Spacetime Dipole Wave Pressure And Black Holes A New Way To Obtain The Schwarzschild Metric, Without Using General Relativity Field Equations." *Asian Journal Of Mathematics And Physics*, Volume 2013, Article ID amp0107, 15 pages. ISSN 2308-3131. [2309.0090v1.pdf \(vixra.org\)](https://vixra.org/pdf/2309.0090v1.pdf)
- [26] Ulianov P. Y. (2013) "An Alternative to the Higgs field Mass Generation Mechanism based on a Dipole Wave Pressure Model." *Asian Journal Of Mathematics And Physics*. Volume 2013, Article ID amp0084, ISSN 2308-3131. <https://vixra.org/abs/2308.0200>
- [27] Ulianov, P. Y. (2016). "Breaking the Paradigm of Negative Mass: Why Newton's Second Law Needs to Be Modified to Enable Newton's Gravitational Law to Deal with Antimatter." *Global Journal of Physics Vol*, 4(1). <https://hal.science/hal-04231878>
- [28] Ulianov, P. Y., & Negreiros, J. P. (2015). "Does the value of Planck time vary in a Black Hole Event Horizon? A new way to unify General Relativity and Quantum Mechanics." *Global Journal of Physics*, 3(1), 165-171. <https://vixra.org/abs/2309.0096>
- [29] Ulianov, P. Y. (2013). "An alternative to the Higgs field mass generation mechanism based on a dipole wave pressure model." *Asian Journal of Mathematics and Physics*, 2013. <https://vixra.org/pdf/2308.0200v1.pdf>
- [30] Ulianov, P. Y. (2023). "Ulianov Perfect Liquid Model Explaining why Matter Repels Antimatter." <https://vixra.org/pdf/2308.0199v1.pdf>
- [31] Ulianov, P. Y., Mei, X., & Yu, P. (2016). "Was LIGO's Gravitational Wave Detection a False Alarm?". *Journal of Modern Physics*, 7(14), 1845. https://www.scirp.org/html/1-7502879_71246.htm
- [32] Mei, X., Huang, Z., Ulianov, P. Y., & Yu, P. (2016). "LIGO Experiments Cannot Detect Gravitational Waves by Using Laser Michelson Interferometers-Light's Wavelength and Speed Change Simultaneously When Gravitational Waves Exist Which Make the Detections of Gravitational Waves Impossible for LIGO Experiments". *Journal of Modern Physics*, 7(13), 1749-1761, <https://www.scirp.org/journal/paperinformation.aspx?paperid=70953>
- [33] Ulianov, P. Y. (2016). "How Can We Observe Waves Without Seeing The Ocean?" <https://vixra.org/abs/2308.0042>
- [34] Policarpo, Y. U. (2023) "21 Century, the True / Fake Age. A True Artificial Intelligence Analyses a Fake Gravitational Wave Detector". <https://hal.science/hal-04231882>
- [35] Ulianov, P. Y. (2023). Excel Table, with all dataset, calculations and graphics, presented in this article, <https://docs.google.com/spreadsheets/d/1ZF2dV8ps5z63TDWFZSrZVye4-S4MJJKk/edit?usp=sharing&oid=116104128331295516455&rtpof=true&sd=true>